



# Experimental study of concrete creep under thermal-mechanical-hydric conditions

Yue Liang · Wei Chen · Nicolas Burlion · Jianfu Shao 

Received: 24 July 2020 / Accepted: 29 January 2021 / Published online: 15 February 2021  
© RILEM 2021

**Abstract** In this paper, the creep deformations of two representative concrete materials are investigated under thermal-mechanical-hydric conditions. Both basic and drying creeps are considered. Triaxial compression creep tests are first performed under a confining pressure of 5 MPa and three different values of temperature ( $T = 20\text{ }^{\circ}\text{C}$ ,  $50\text{ }^{\circ}\text{C}$  or  $80\text{ }^{\circ}\text{C}$ ). Two different levels of differential stress are considered (50% and 80% of the peak strength at  $20\text{ }^{\circ}\text{C}$ ). These tests are used for the characterization of basic creep. Then hydric creep tests are conducted on samples subjected to uniaxial compression condition with different prescribed values of axial stress (30%, 50% and 70% of the uniaxial compressive strength) and at constant temperature ( $20\text{ }^{\circ}\text{C}$ ). The samples are progressively dried by decreasing the relative humidity (RH) from 98 to 50%. The relative variations of sample mass are also measured during the drying process. It is found that the basic creep strain rate is enhanced by temperature and differential stress. The drying kinetics is strongly influenced by the

compositions of concrete. The drying creep deformation is directly correlated with the mass loss kinetics.

**Keywords** Basic creep · Drying creep · Temperature · Concrete · Thermo-hydric-mechanical coupling

## 1 Introduction

This study is carried out in the framework of research projects coordinated by Andra (French National Agency for the Management of Radioactive Waste) on typical concretes envisaged for the underground storage of radioactive waste. In this context, concretes will be subjected to complex environmental conditions including mechanical loading, temperature variation, desaturation and resaturation and chemical degradation [1, 2]. Indeed, concrete materials are used as engineering barrier or supporting structures are subjected to complex stress paths due to interactions with the geological barrier and the swelling clay also used as engineering barrier. Further, concrete components can be desaturated by ventilation in galleries and resaturated by water from the surrounding geological formation. On the other hand, the heat produced by exothermal radioactive waste can induce significant variation of temperature. Finally, various chemical degradation process such as leaching and carbonation

---

Y. Liang · W. Chen  
School of Civil Engineering, Architecture and Environment, Hubei University of Technology (HBUT), NO. 28, Nanli Road, Hong-shan District, Wuhan, P.R. China

N. Burlion · J. Shao (✉)  
University of Lille, CNRS, Centrale Lille, LaMcube, UMR9013, 59000 Lille, France  
e-mail: jian-fu.shao@polytech-lille.fr

can also take place. The thermo-hydro-mechanical (THM) behaviors of concretes are strongly influenced by these coupled environmental conditions.

The feasibility of geological disposal of radioactive waste requires the characterization of long term THM behaviors of all involved materials in the storage facilities including concretes, ranging from a few thousands to a few tens of thousands of years. It is known that all concrete materials exhibits creep deformation of various origin. It is therefore crucial to perform experimental and modeling studies on the creep deformation of concrete under complex environmental conditions as mentioned before.

Concrete creep behavior has been studied for a long time, many experiments have been carried out to measure creep and study different influencing variables. These variables include W/C ratio [3–5], relative humidity [6–11], types of cement [12], additions used [13–18], etc. Concerning the same context of geological disposal of radioactive waste, some authors have performed studies on basic creep deformation of concrete at three different values of temperature, 20 °C, 50 °C and 80 °C [19, 20]. It was shown that the creep deformation increased exponentially with temperature and that the thermal damage occurred beyond 50 °C, revealed by a decrease in the elastic modulus. With regard to the effects of humidity, previous studies have mainly focused on the drying induced shrinkage under constant humidity. When concrete is subjected to simultaneous drying and mechanical loading, the resulting deformation is much greater than the sum of the basic creep and the drying shrinkage [21, 22]. Many other studies were devoted to understanding the physical mechanisms involved in drying creep such as micro-cracking and shrinkage [23–35]. In the underground storage structures, the concrete components can be subjected to important hydric cycles, temperature variations and multi-axial mechanical loading. Many studies indicated that the behavior of concrete under varying relative humidity because swelling occurs when the water content increases [36–39]. Some previous have also been devoted to the characterization and modeling of temperature and damage effects on the basic creep deformation of concrete [40–43].

However, few studies have been performed on the characterization of creep deformation of concretes under coupled thermal-mechanical-hydric conditions. This is the main objective of this study. A new series of

laboratory tests are performed on two types of concretes respectively fabricated with CEM I and CEM V cements according to European norms. For each material, both basic and drying creeps are considered. For this purpose, triaxial compression creep tests are first carried out under three different values of temperature and two levels of differential stress. The obtained results are used to investigate the effects of temperature and stress level on the basic creep deformation of two tested materials. Then drying tests are performed under different values of uniaxial compression stress to evaluate the effects of mechanical load on the drying kinetics and drying induced creep deformation. For two groups of tests, the influences of concrete compositions on both basic and drying creep deformations are also analyzed.

## 2 Experimental program

### 2.1 Materials

Two sets of reference materials are suggested by Andra and considered in this study. Their main difference lies in the nature of the cement used in the formulation, respectively CEM I and CEM V/A. The CEM I type is made of pure Portland cement, while the CEM V/A cement is constituted of 60% clinker in mass, 22% blast-furnace slag, 14% fly ash and 4% setting regulator. After the extraction from mold, both concretes are cured in lime-saturated water (20 °C) for about six months until the tests were performed. All the samples have almost the same curing duration. In Table 1, one presents the detailed formulations of the CEM I and CEM V/A concretes. In Table 2, the basic physical and mechanical properties of the two concretes are given. These two materials are chosen for potential use in the structures for geological disposal of radioactive waste due to their low porosity and permeability as well as suitable mechanical properties.

Cylindrical samples are used in this study. The diameter of samples is 36.5 mm and the height is 69 mm for basic mechanical creep tests and 120 mm for drying creep tests. The size of samples is considered as large enough as a Representative Elementary Volumes (REV) with respect to the size of the largest aggregate, namely 12 mm.



**Table 1** Formulations of two studied concretes

Constituents	CEM I (kg/m <sup>3</sup> )	CEM V/A (kg/m <sup>3</sup> )
Cement: CEM I 52.5	400	
Cement: CEM V/A 42 ,5N		450
Sand 0/4	858	800
Gravel 5/12.5	954	984
Superplasticizer glenium 27	10	2.5
Water	171	176.3
W/C	0.43	0.39

**Table 2** Basic physical and mechanical properties of two concretes

Properties	CEM I	CEM V/A
Uniaxial compressive strength 3 months	66.6 MPa	66.2 MPa
Young's modulus 3 months	23.9 GPa	23 GPa
Poisson's ratio 3 months	0.16	0.26
Porosity	8.2%	12.4%

## 2.2 Testing program

It is worth noticing that in general four complementary and interacting creep and shrinkage processes are identified in concrete materials, namely autogenous and drying shrinkage, basic and drying creep. Further, the variation of temperature can also induce thermal deformation of materials. In this study, there are two objectives. The first one is to investigate the influences of temperature and mechanical stress on the basic creep deformation and the second one is to study the effect of mechanical loading on the drying creep process. The autogenous or drying shrinkage as well as the thermal deformation is subtracted from total deformation and is not specifically studied here. For this purpose, two sets of laboratory tests are carried out.

The first set is devoted to the basic creep behavior. The objective is to evaluate the impact of multi-axial stress and temperature on the kinetics of creep deformation. Triaxial compression creep tests are performed under a confining stress of 5 MPa. A preliminary triaxial compression test is first conducted at 20 °C to identify the peak differential (also called deviatoric) stress for this confining stress. Based on this reference strength, creep tests are performed under three different values of temperature: 20 °C, 50 °C and 80 °C. For each temperature, two levels of differential stress are used, respectively at 50% and 80% of the peak strength. The temperature is prescribed to the

desired value after the application of confining stress. The thermal deformation is measured but not specifically quantified here. When the thermal deformation reaches its stationary value, the differential stress is applied. The instantaneous deformation is first measured and the creep stage is then started. The emphasis is put on the evolution of the deformation with time after subtracting the thermal and instantaneous strains.

The second set focuses on the drying creep behavior. To this end, uniaxial compression creep tests are performed at 20 °C and with drying process. For each kind of concrete, three tests are simultaneously conducted: the samples are first subjected to three different levels of axial stress, respectively at 30%, 50% and 70% of the uniaxial compression strength. Then, under the constant prescribed stress, the samples are progressively dried from the saturated state to partially saturated one by decreasing step by step the relative humidity to 98%, 95%, 90%, 70% and 50%. At each drying step, the relative mass variations and the evolutions of axial strain of all samples are measured, in order to characterize the effect of stress on the drying process. The mass variations are measured with an accuracy of  $\pm 0.1$  g.

## 2.3 Experimental devices

The triaxial creep tests are carried out by using the self-compensated autonomous cell presented in Fig. 1. Unlike classical triaxial cells, the piston of the cell is

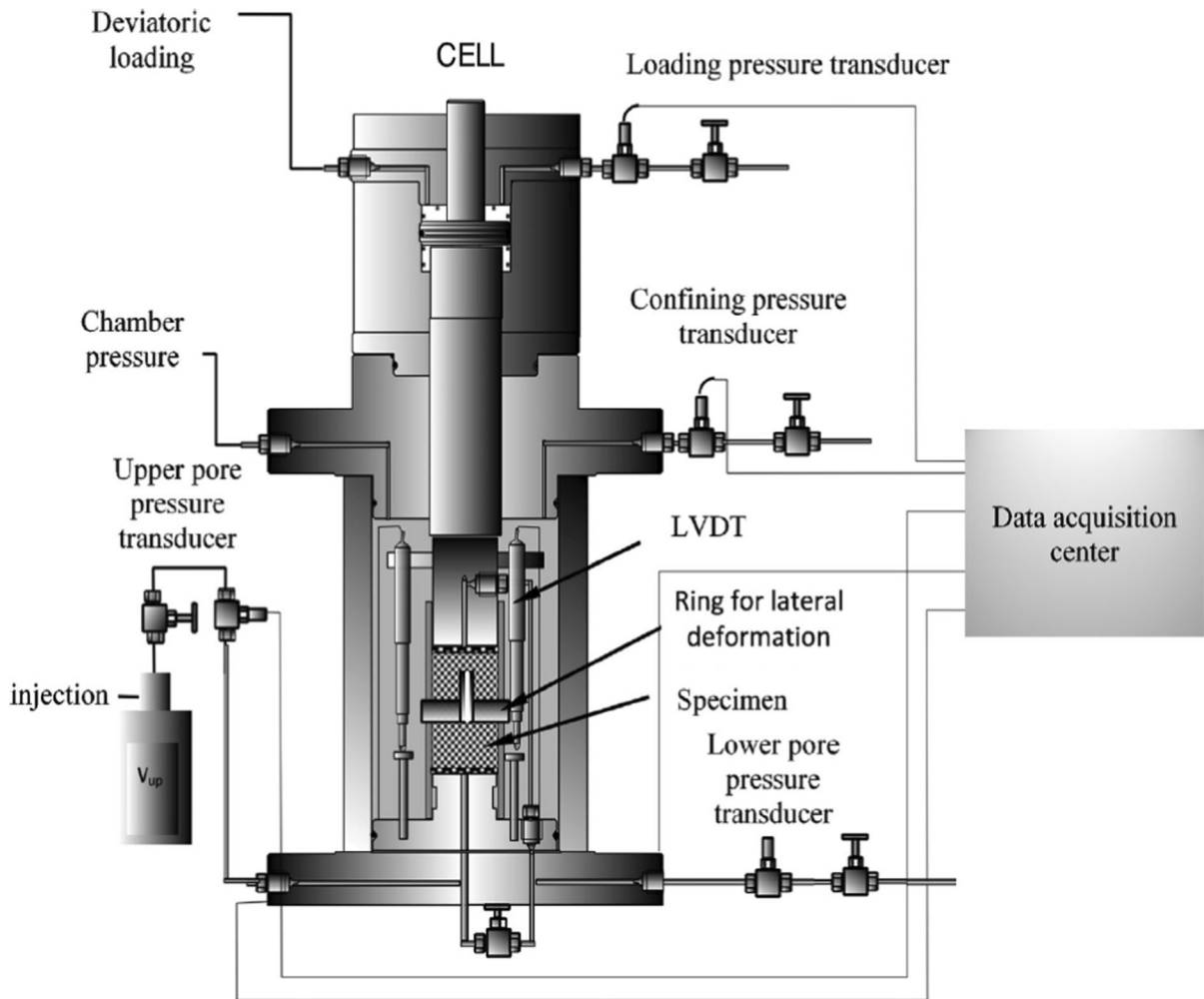


**Fig. 1** Experimental setup sketch for triaxial creep tests

not subjected to the upward axial force induced by confining pressure. For tests under controlled temperature, the whole cell is placed inside an oven equipped with an electronic temperature controller and a fan to homogenize the temperature inside the oven. This type of oven provides an accuracy of about  $\pm 0.3$  °C for temperature and allows maintaining the entire cell at the desired value of temperature. Three pressure sensors are used respectively for monitoring confining stress, axial stress and pore fluid pressure. Longitudinal displacement is measured by two LVDTs while circumferential strain by a collar. These instruments are connected to an electronic data acquisition chain which is located outside the oven.

As shown in Fig. 1, the two LVDTs for the longitudinal displacement are fixed on the loading

platens. Therefore, one measures the global displacement of system including the interfaces between sample and loading platens. To avoid the strain affected by interfaces the between the sample and the loading platens. In order to minimize the effect of the interfaces, the end surfaces of sample are carefully rectified and polished until a good contact is obtained between the sample end surfaces and platens. Even with this precaution, the axial strain measured by using LVDTs is generally higher than that by strain gauges. However, due to high values of temperature and strong variations of relative humidity, the use of strain gauges is very delicate for long duration creep tests. This is the reason that LVDTs is preferred in the present study.

The experimental device designed for uniaxial drying creep tests contains a loading frame. This one is composed of four tie-rods and two plates. Between the two plates are placed an analogic force sensor, the sample and a ball joint. Two collars are placed respectively at 1/3 and 2/3 of the height of the sample, between which the axial displacement is measured, as shown in Fig. 2a. A comparator is also fixed to the first collar and the feeler of this comparator comes into contact with the second collar.

To ensure that the load is correctly applied along the central axis of the system, a centering mark is indicated on the lower plate to install the pressure gauge. Thus, the value indicated by the pressure gauge well represents the force exerted on the tested sample. According to the testing program presented above, 12 loading frames are used simultaneously (6 for each kind of concrete) and they are placed in a Binder climatic chamber, as shown in Fig. 2b, by regularizing the temperature around 20 °C and prescribing the desired relative humidity. Nitrogen gas is added to the enclosure at the end of the each measurement for about ten minutes to avoid carbonation of the materials.

During the uniaxial drying creep tests, the variation of the mass of each frame is measured with a balance of an accuracy of 0.05 g. This is done outside the climatic chamber during a short time of about 20 min so that the perturbations induced by the external environmental conditions on the creep deformation can be neglected. Further, it is assumed that the variation in mass of each frame is due to the tested concrete sample only.

### 3 Experimental results and discussions

#### 3.1 Triaxial creep tests

The triaxial creep tests are performed on the CEM-I concrete samples with two loading steps and at three different values of temperature as defined above. The confining pressure is kept to 5 MPa during the creep steps. Moreover, at each loading step, three unloading and reloading cycles are realized in order to measure the elastic properties. As an example, in Fig. 3, the global stress-strain curves of the test conducted at 20 °C are presented. It is found that the hysteresis loops are slightly larger under 80% of the peak strength than that under 50%. As the hysteresis loops are generally related to the material viscosity and frictional sliding along inclined micro-cracks, it seems that these two mechanisms are enhanced by the differential stress level. On the other hand, in spite of the hysteresis loops observed, the secant values of Young's modulus and Poisson's ratio are still measured from the unloading and reloading points of each cycle. The obtained values are summarized in Table 3, for three levels of temperature. One can see that the elastic properties do not show significant differences between the different values of temperature and differential stress. However, in detail, one can still observe that under 50 °C and 80 °C, the Young's modulus is smaller when the differential stress is higher. This reduction of elastic stiffness can be attributed to an induced damage of samples by the differential stress. At the same time, the elastic modulus does not change between three cycles

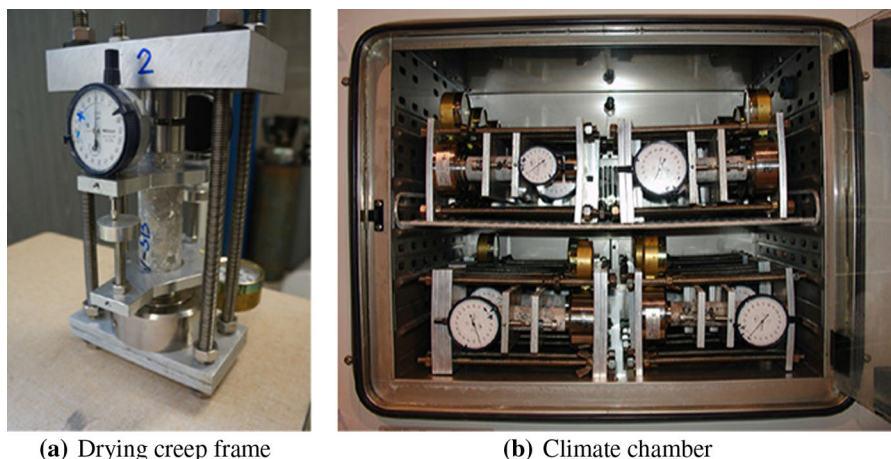


**Fig. 2** Experimental setup for drying creep tests

**Fig. 3** Axial and lateral strains versus differential stress during the triaxial creep test at 20°C and under a confining pressure of 5 MPa

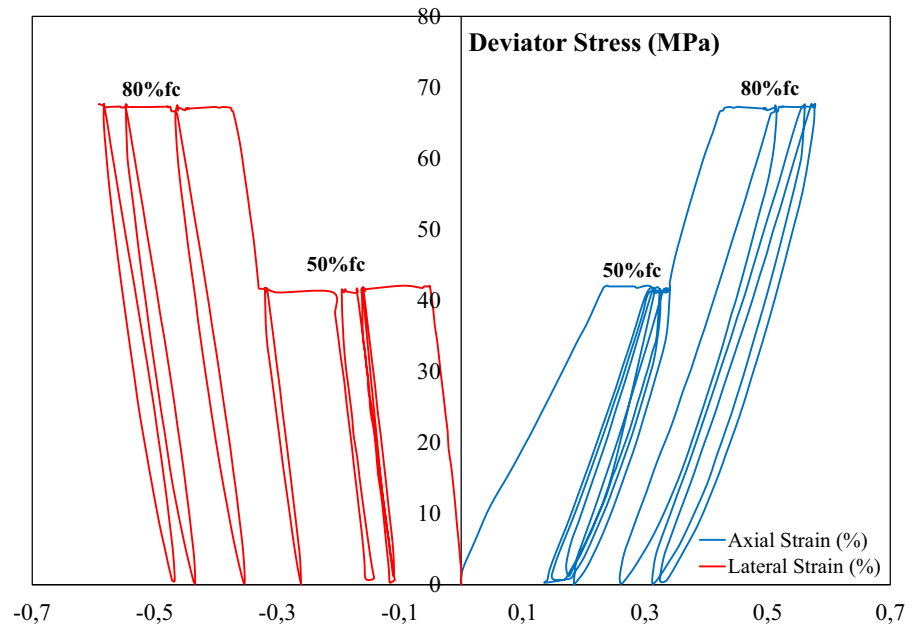


**Table 3** Young's modulus and Poisson's ratio of CEM-I concrete measured during the triaxial creep tests (3 measurements for each of the two loading steps)

		Young's modulus (GPa)			Poisson's ratio		
20 °C	50% fc	25.3	25.2	27	0.35	0.35	0.37
	80% fc	25.7	26.6	26.6	0.45	0.47	0.49
50 °C	50% fc	27.3	27.6	27.6	0.31	0.31	0.32
	80% fc	25	24.9	24.8	0.37	0.43	0.49
80 °C	50% fc	27.9	28.7	28.8			
	80% fc	25	26.4	26.2			

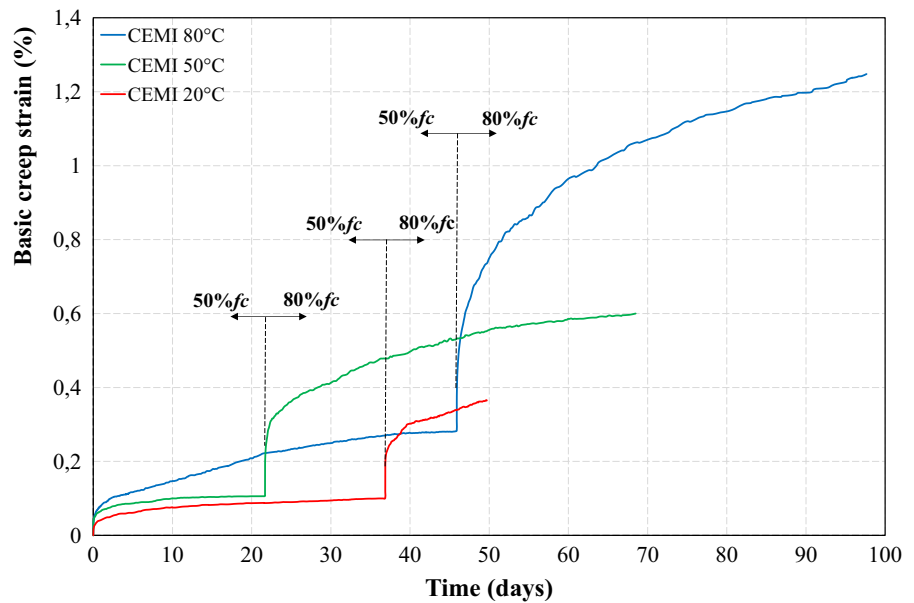
during each creep step. Therefore, the material damage is mainly controlled by the differential stress rather than the creep process. On the other hand, the values of Poisson's ratio increase slightly between three cycles. This increase is even bigger when the differential stress is higher. It seems that the value of Poisson's is enhanced by the creep deformation. Moreover, it is observed that the values of Young's modulus obtained in this study seem to be relatively small for this types of concretes. This could be due to the fact that the axial strain measured by using LVDTs is slightly overestimated, as explained above.

In Fig. 4, the variations of axial creep strain with time are presented for three triaxial creep tests

performed respectively at 20 °C, 50 °C and 80 °C on the CEM-I concrete samples which are subjected to two levels of differential stress. The instantaneous strains generated by the applied differential stress are subtracted from the total ones in this Figure. The time axis denotes the duration of creep phases without that used for the loading of differential stress. On the other hand, the autogenous shrinkage is also an important feature and related to time-dependent deformation of concrete. In general, the autogenous shrinkage is measured on sealed saturated sample during six months and the maximum value reaches around 71 days. In the present study, all tested samples were conserved in water during six months. It is assumed that the autogenous shrinkage was almost completed before the beginning of tests and its effect on the measured creep deformation can be neglected.

According to the results shown in Fig. 4, it is obvious that when the differential stress is maintained at the same level of differential stress, for instance 50% of the peak strength, the creep strain of concrete is larger when the temperature it higher. It seem that the temperature amplifies the creep deformation of the CEM-I concrete, as it was shown in some previous studies [19, 29]. On the other hand, when the differential stress is raised to 80% of the peak strength during the second loading step, the creep strains are clearly higher than those during the first loading step

**Fig. 4** Evolutions of total axial strain with time of CEM-I concrete in triaxial creep tests at 20 °C, 50 °C and 80 °C



under 50% of the peak strength for all three values of temperature. Therefore, the differential stress level significantly enhances the creep deformation of the concrete. At the same time, like in the first loading step, the creep strain is again larger when the temperature is higher.

In order to get a deep characterization of creep deformation kinetics of the CEM-I concrete, the creep strain rates are calculated from the accumulated total strains by subtracting the elastic strains caused by the applied stress increments during the two loading steps. The evolutions of creep strain rate with time are respectively presented in Fig. 5 for 50% of the peak strength and in Fig. 6 for 80% of the peak strength and three values of temperature. It is found that for the two loading steps and all values of temperature, the creep strain rates decrease quickly during the first period of creep, for example of about 10 h. The creep strain rates evolve towards some stationary values without completely vanishing until the end of each loading step. It indicates that the creep deformation is not fully stabilized at the end of each loading step. From these results, it is clear that the creep strain rate is larger when the temperature is higher, almost during all the creep periods. The curve for the case at 50 °C and under 50% of the peak strength in Fig. 5 is slightly apart from the general trends. This should be rather related to experimental disparity.

### 3.2 Drying creep tests

The uniaxial drying creep tests are performed on the two kinds of concretes, CEM-I and CEM-V, following the experimental procedure presented above. The emphasis is here put on the evolution of drying creep strain. The drying shrinkage is thus subtracted from the total deformation measured in the tests.

In Fig. 7, the relative mass variations with time during the different drying steps are presented for the samples of two concrete subjected to the different values of axial stress. The relative mass loss is calculated with respect to the reference weight in the saturated state. Each point represents the average value of two tested samples to ensure the representativeness of the results.

At first sight, the drying kinetics of the CEM-I is much higher than that of the CEM-V. At the same time, according to Table 2, the total porosity of CEM-V/A (12.4%) is higher than that of the CEM-I (8.2%). This apparent contradictory result can be explained by the difference of pore size distribution between the two concretes. The results obtained from Mercury Intrusion Porosimetry (MIP) are shown in Fig. 8. In particular, in the previous study reported in [2], the authors have investigated the effect of temperature on the water retention properties of the CEM-I and CEM-V. The materials used in that study were manufactured with the identical formulations to those in this study.

**Fig. 5** Evolutions of creep strain rate of CEM-I concrete under 50% of peak strength in triaxial creep tests with different values of temperature

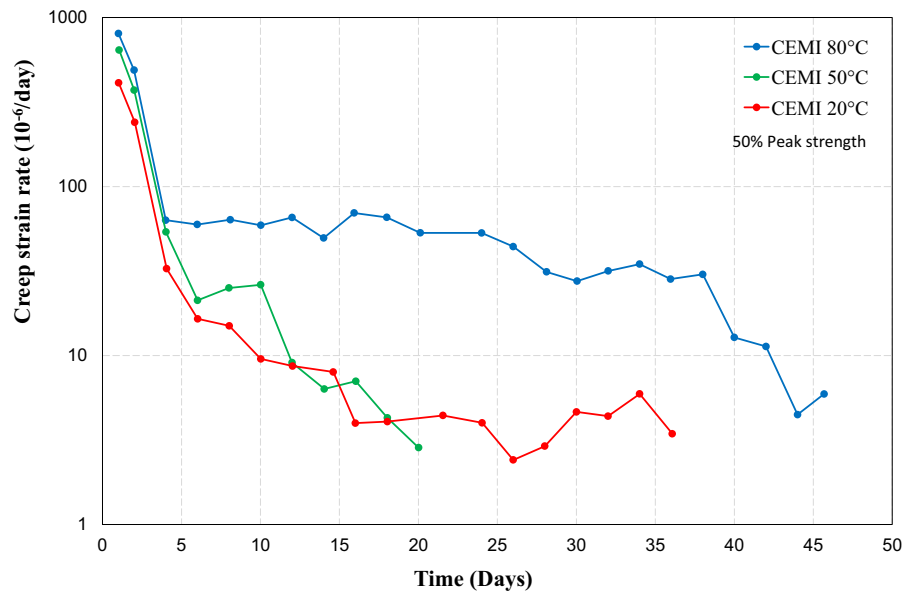
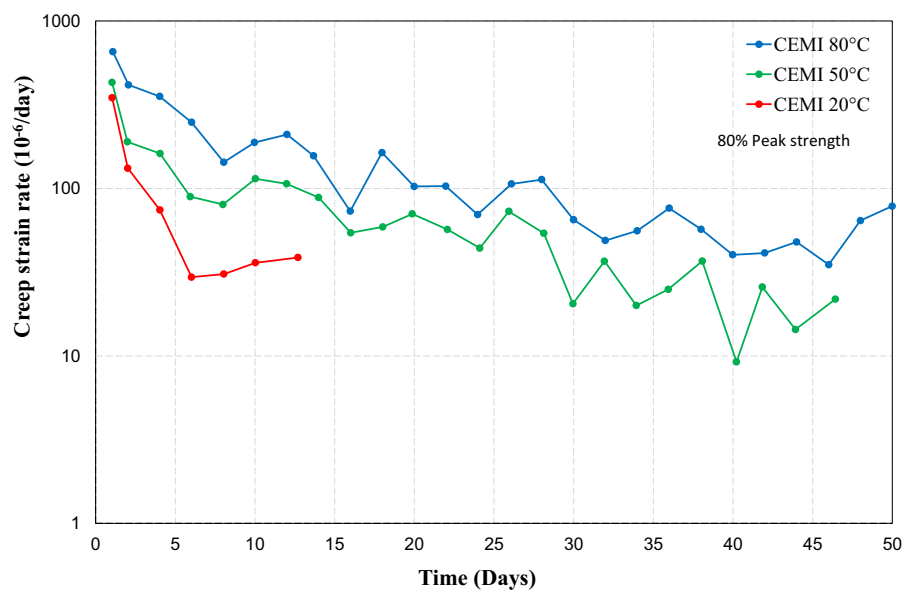


**Fig. 6** Evolutions of creep strain rate of CEM-I concrete under 80% of peak strength in triaxial creep tests with different values of temperature



The CEM-I concrete porosity was of 8.1% and that of the CEM-V was of 11.9%. They have found that the water retention capacity of the CEM-V was greater than the CEM-I, although the CEM-V had a higher porosity than the CEM-I. This was due to the fact that the CEM-V had a larger amount of fine pores than the CEM-I. This difference was attributed to pozzolanic additions in the CEM V/A-type cement, leading to the formation of a greater amount of C-S-H than in the CEM-I. The main difference between the two

concretes lies at the right end of the MIP pore size distribution. For instance, at a diameter of 6 nm (which is the lowest value measurable by the MIP used), the CEM-V presents a cumulated intruded volume of 0.018 ml/g (with a slope increasing towards lower radii), whereas that of the CEM-I is equal to 0.002 ml/g only (with a decreasing slope towards lower radii). This indicates that the CEM-V concrete seems to have significantly more of the narrowest gel pores of C-S-H, than the CEM-I. Besides, the tortuosity of pore



**Fig. 7** Relative mass variations of tested samples of two concretes subjected to different values of axial stress at 20 °C

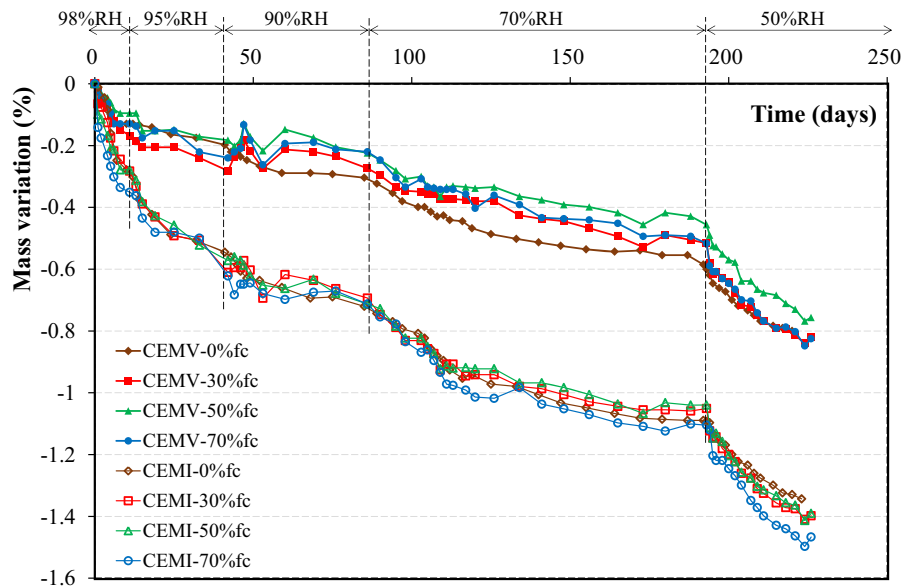
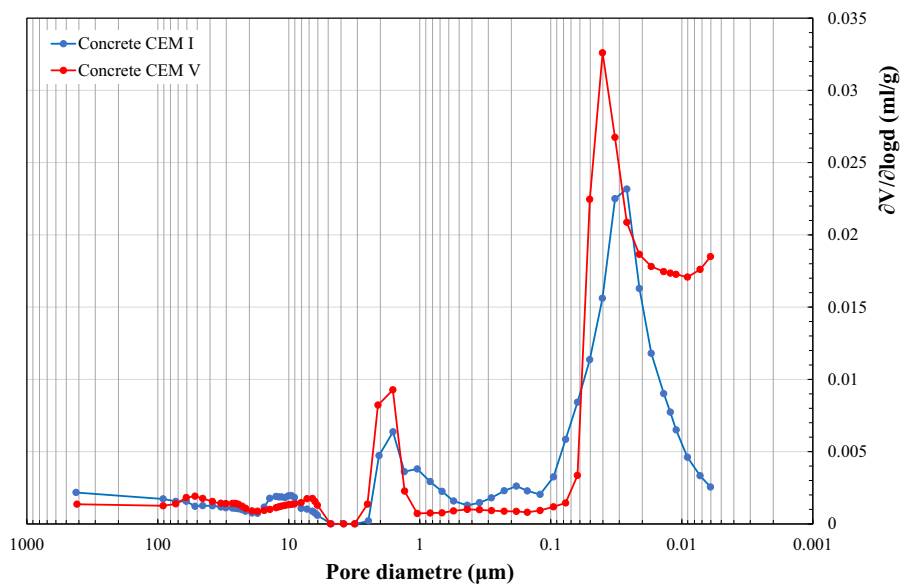


**Fig. 8** Distributions of pore size in CEM-I and CEM-V/A concretes



networks can also affect the drying process, in particular for the case of CEV-V. In our study, the emphasis was put on the effects of temperature, stress and related humidity. It is considered that the thermal-hydric-mechanical coupling can modify the water transport paths of concrete by the creation of micro-cracks for instance and then plays an dominant role in the drying kinetics. However, the effect of tortuosity should be investigated in future works.

There are small differences on the relative mass variation between the CEM-I concrete samples subjected to different axial stresses. It seems that the drying kinetics of CEM-I concrete is little influenced by the loading stress, even at 70% of the compressive strength. For a given hydric gradient, the drying kinetics is mainly by the concrete permeability which can be affected by the closure of initial micro-cracks or the creation of new micro-cracks by the axial stress. In the present case, it seems that the effect of axial

stress on the cracking process in the CEM-I samples is not significant. The results of the present study are consistent with those obtained in some previous works on a mortar with  $W/C = 0.5$  and dried at an age of 28 days [44–46]. On the other hand, the influence of stress level on the drying kinetics seems to be more significant for the CEM-V concrete. However, it is not easy to draw a definite conclusion on this aspect. Indeed, the drying kinetics of the samples without stress ( $\% f_c$ ) is larger than the three others subjected to different axial stresses. This probably suggests that the samples of CEM-V/A contain a number of initial micro-cracks which enhance the drying process. When the samples are compressed by the axial stress, some micro-cracks are closed. Thus, the drying kinetics of the samples under 30% and 50% of uniaxial compression strength are sequentially smaller than that of the stress-free samples. However, when the axial is higher enough, for instance 70% of compression strength, new micro-cracks can be generated as pointed out in [47], facilitating the drying process. There is a competition between the closure of initial cracks and the creation of new ones. As a consequence, the drying kinetics of the samples under 70% is larger than that under 50% but smaller than that under 30%.

Finally, from Fig. 7, one can clearly observe that the drying kinetics is significantly accelerated when the relative humidity is lower than 50%. This is directly related to the nucleation and propagation of cracks induced by the drying shrinkage. According to some previous studies, In addition, the migration of water in concretes can be significantly enhanced if the aperture of induced cracks exceeds a few tenths of a millimeter [48, 49]. Based on the observations obtained using a fluorescent optical microscope and a scanning electron microscope (SEM) on mortar samples subjected to drying process [50–52], the aperture of the drying shrinkage induced cracks typically ranged between 0.25 and 50  $\mu\text{m}$ .

Throughout the five different steps of drying, the time-dependent axial strains of the tested samples are measured. The obtained results are presented Fig. 9. One can firstly remark que for all the samples, there is a sudden increase of drying rate at the beginning of each step when the relative humidity is decreased. This sudden increase is more and more significant when the relative humidity is lower than 70%. On the other hand, at each drying step, the tangent slope of drying creep strain curve is continuously decreasing. It

seems that the axial creep strain evolves towards an asymptotic stationary value. However, this should be confirmed by additional tests with longer drying duration.

By comparing the strains obtained for the two different concretes, some interesting results can be obtained. For the samples subjected to 70% of compression strength, the drying induced strain of the CEM-I is clearly higher than that of the CEM-V/A. This is consistent with the relative mass loss presented in Fig. 7. But for the samples under 50% of compression strength, the two concretes have almost the same evolutions of strain. And for the samples under 30% of strength, the drying induced strain of the concrete CEM-I is even than smaller than that of the concrete CEM-V/A. The results for these two levels of loading are obviously not in agreement with the drying kinetics shown in Fig. 7.

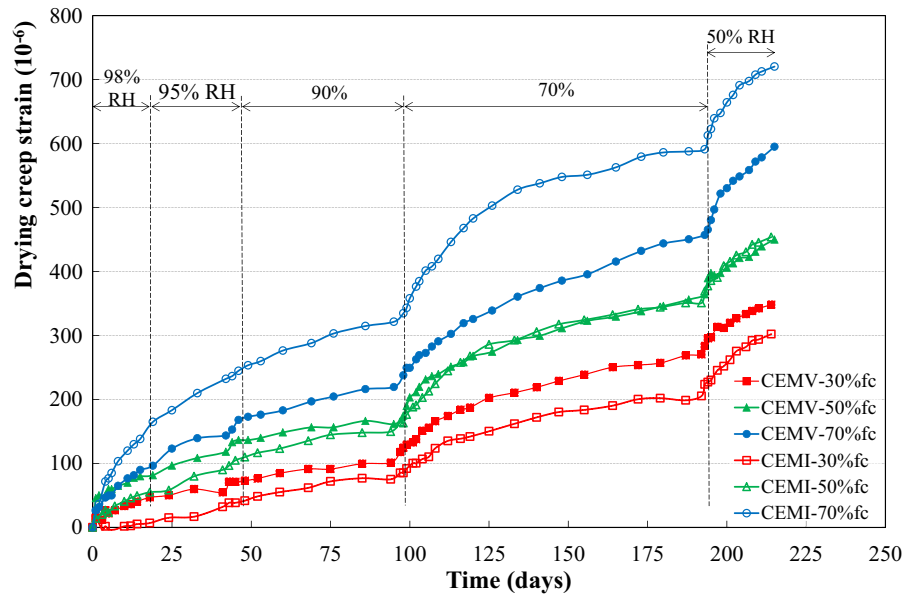
Actually, the strains measured during the five drying steps are attributed to two superposed mechanisms, respectively related to the mechanical creep deformation of concretes induced by the applied axial stress and to the drying shrinkage deformation. According to the results obtained, it seems that the mechanical creep deformation induced by the axial stress of the concrete CEM-V/A at lower stress loading levels, for instance 30% and 50% of compression strength, is more important than that of the CEM-I. As a consequence, even if its the drying kinetics is lower than that of the CEM-I, its total creep strains are higher than those of the CEM-I. However, at the stress level of 70%, the mechanical creep deformation of the CEM-I is obviously intensified. Combined with the higher drying kinetics, the total creep strain of the CEM-I is much larger than that of the CEM-V/A.

#### 4 Conclusions

In this study, the basic and drying creep behaviors of two representative concretes have been investigated both under thermal, mechanical and drying conditions. A series of new experimental results have been obtained and they are useful for the optimal design of facilities for the geological disposal of radioactive waste. Based on the results obtained, some key remarks can be formulated.



**Fig. 9** Evolutions of axial strain with time during five drying steps of the tested samples of two concretes at 20 °C



The basic mechanical creep deformation of CEM-I concrete is significantly amplified by the raise of temperature, which accelerates the sliding of CSH sheets and decreases the viscosity of cement paste. At the same time, the basic creep deformation is also significantly enhanced by the prescribed stress level. However, no creep-induced failure of samples was observed until the applied differential stress reached 80% of the peak strength. On the other hand, no significant effects of temperature, loading level and creep process were obtained on the elastic properties of the concrete.

A large difference of drying kinetics has been obtained between the two studied concretes. The rate of mass loss is much higher for the CEM-I concrete than for the CEM-V/A. The drying kinetics of the CEM-I was almost not affected by the applied axial stress while that of the CEM-V/A slightly influenced. For the latter material, there is a competition between the closure of initial micro-cracks and the nucleation of new ones. This makes the drying kinetics of the CEM-V/A dependent on the applied stress level.

The time dependent strains of two concretes in coupled stress-drying conditions are driven by both the mechanical creep deformation and the drying shrinkage process of materials. The mechanical creep strains of the CEM-V/A under low stress levels are much larger than those of the CEM-I. However, the mechanical creep deformation of the CEM-I is

significantly accelerated when the applied stress becomes high, as confirmed in the basic triaxial creep tests. However, only one confining pressure was considered in each type of creep tests. It was not possible to characterize the effect of confining stress on both the basic and drying creeps. This feature should be investigated in future studies.

The experimental results obtained from the present study provide a useful data base for developing theoretical and numerical modeling of time-dependent behavior of concrete structures under coupled thermal-mechanical and hydric conditions. This will be the subject of our ongoing studies.

**Acknowledgements** This work was jointly funded by Andra (French National Agency for radioactive waste management, contract GLciment-545-0608), the National Natural Science Foundation of China (Grant: 51709097) and Hubei Provincial Natural Science Foundation of China (Grant: 2017CFB604).

#### Compliance with ethical standards

**Conflict of interest** The authors declare that they have no conflict of interest.

#### References

- Andra (2012) Referentiel Materiaux 2012 CG.RP.ASCM. 12.0014
- Brue F, Davy CA, Skoczylas F, Burlion N, Bourbon X (2012) Effect of temperature on the water retention

- properties of two high performance concretes. *Cem Concr Res* 42:384–396
3. Kovler K (1995) Interdependence of creep and shrinkage for concrete under tension. *J Mater Civil Eng* 7:96–101
  4. Smadi MM, Slate FO, Nilson AH (1987) Shrinkage and creep of high-medium and lowstrength concretes, including overloads. *ACI Mater J* 84:224–234
  5. Shen D, Jiang J, Wang W, Shen J, Jiang G (2017) Tensile creep and cracking resistance of concrete with different water-to-cement ratios at early age. *Constr Build Mater* 146:410–418
  6. Bazant ZP, Hemann JH, Koller H, Najjar LA (1973) Thin-wall cement paste cylinder for creep test at variable humidity or temperature. *Mater Struct* 6:1–34
  7. Bazant ZP, Asghari AA, Scamiot J (1976) Experimental study of creep of hardened Portland cement paste at variable water content. *Mater Struct* 9:279–290
  8. Pihlajavaara SE (1974) A review of some of the main results of a research on the aging phenomena of concrete: effect of moisture conditions on strength, Shrinkage and creep of mature concrete. *Cem Concr Res* 4:761–771
  9. He ZH, Qian CX (2011) Internal relative humidity and creep of concrete with modified admixtures. *Prog Nat Sci Mater Int* 21:426–432
  10. Frech-Baronet J, Sorelli L, Charron JP (2017) New evidences on the effect of the internal relative humidity on the creep and relaxation behaviour of a cement paste by micro-indentation techniques. *Cem Concr Res* 91:39–51
  11. Nastic M, Bentz EC, Kwon OS, Papanikolaou V, Tchnerer J (2019) Shrinkage and creep strains of concrete exposed to low relative humidity and high temperature environments. *Nucl Eng Des* 352:110154
  12. Benboudjema F (2002) Modelisation des deformations differees du beton sous sollicitations biaxiales. Application aux enceintes de confinement de batiments reacteurs des centrales nucleaires. Doctoral thesis, Universite de Marne la Vallee. 2002, p 258
  13. Khatri RP, Sirivivatnanon V (1995) Effect of different supplementary cementitious materials on mechanical properties of high-performance concrete. *Cem Concr Res* 25:209–220
  14. Jianyong L, Yan Y (2001) A study on creep and drying shrinkage of high-performance concrete. *Cem Concr Res* 31:1203–1206
  15. Pane I, Hansen W (2002) Early age creep and stress relaxation of concrete containing blended cements. *Mater Struct* 35:92–96
  16. Klausen AE, Kanstad T, Bjontegaard O, Sellevold E (2017) Comparison of tensile and compressive creep of fly ash concretes in the hardening phase. *Cem Concr Res* 95:188–194
  17. Gayarre FL, Gonzalez JS, Perez CLC, Serrano Lopez MA, Ros PS, Martinez-Barrera G (2019) Shrinkage and creep in structural concrete with recycled brick aggregates. *Constr Build Mater* 228:116750
  18. Mohammadhosseini H, Alyousef R, Lim NHAS, Tahir MM, Alabduljabbar H, Mohamed AM (2020) Creep and drying shrinkage performance of concrete composite comprising waste polypropylene carpet fibres and palm oil fuel ash. *J Build Eng* 30:101250
  19. Ladaoui W, Vidal T, Sellier A (2011) Effect of a temperature change from 20 to 50 °C on the basic creep of HPC and HPFFC. *Mater Struct* 44:1629–1639
  20. Ladaoui W, Vidal T, Sellier A, Bourbon X (2013) Analysis of interactions between damage and basic creep of HPC and HPFFC heated between 20 and 80 °C. *Mater Struct* 46:13–23
  21. Pickett G (1942) The effect of change inmoisture-content of the creep of concrete under a sustained load. *J Am Concr Inst* 13:333–356
  22. Wittmann FH, Roelfstra PE (1980) Total deformation of loaded drying concrete. *Cem Concr Res* 10:601–610
  23. Bazant ZP, Xi Y (1994) Drying creep of concrete: constitutive model and new experiments separating its mechanisms. *Mater Struct* 27:3–14
  24. Pihlajavaara SE (1974) A review of some of the main results of a research on the ageing phenomena of concrete: effect of moisture conditions on strength, shrinkage and creep of mature concrete. *Cem Concr Res* 4:761–771
  25. Bazant ZP, Chern JC (1985) Concrete creep at variable humidity: constitutive law and mechanism. *Mater Struct* 18:1–20
  26. L'Hermite R, Mamillan M (1969) Nouveaux resultats et recentes etudes sur le fluage du beton. *Mater Struct* 2:35–41
  27. Bazant ZP (1975) Theory of creep and shrinkage in concrete structures: a precis of recent developments. *Mech Today* 2:1–93
  28. Acker P, Ulm FJ (2001) Creep and shrinkage of concrete: physical origins and practical measurements. *Nucl Eng Des* 203:143–158
  29. Sellier A, Buffo-Lacarriere L, Multon S, Vidal T, Bourbon X (2012) Nonlinear basic creep and drying creep modelling. In: P. Rossi, J.L. Tailhan (Eds.) Strategy for sustainable concrete structures (SSCS Conference). Aix-en-Provence, France, May 29–June 1
  30. Bazant ZP (1978) Solidification theory for aging creep. *Cem Concr Res* 8:601–611
  31. Burlion N, Bourgeois F, Shao JF (2005) Effects of drying on mechanical behaviour of concrete. *Cem Concr Compos* 27:367–379
  32. Benboudjema F, Meftah F, Torrenti JM (2005) Interaction between drying, shrinkage, creep and cracking phenomena in concrete. *Eng Struct* 27:239–250
  33. Yazdizadeh Z, Marzouk H, Hadianfard MA (2017) Monitoring of concrete shrinkage and creep using fiber Bragg grating sensors. *Constr Build Mater* 137:505–512
  34. Su L, Wang YF, Mei SQ, Li PF (2017) Experimental investigation on the fundamental behavior of concrete creep. *Constr Build Mater* 152:250–258
  35. Charpin L, Le Pape Y, Coustabeau É, Toppani É, Heinfing G, Le Bellego C, Masson B, Montalvo J, Courtois A, Sanahuja J, Reviron N (2018) A 12year EDF study of concrete creep under uniaxial and biaxial loading. *Cem Concr Res* 103:140–159
  36. Bazant ZP, Hemann JH, Koller H, Najjar LJ (1973) A thin-wall cement paste cylinder for creep tests at variable humidity or temperature. *Mater Struct* 6:227–281
  37. Bazant ZP, Wu ST (1974) Creep and shrinkage law for concrete at variable humidity. *J Eng Mech Div* 100:1183–1209



38. Torrenti JM, Granger L, Diruy M, Genin P (2011) Modélisation du retrait du béton en ambiance variable. *Rev Fr Génie Civ* 1(1):687–698
39. Bazant ZP (1972) Thermodynamics of hindered adsorption and its implications for hardened cement paste and concrete. *Cem Concr Res* 2:1–16
40. Sellier A, Multon S, Buffo-Lacarrière L, Vidal T, Bourbon X, Camps G (2016) Concrete creep modelling for structural applications: non-linearity, multi-axiality, hydration, temperature and drying effects. *Cem Concr Res* 79:301–315
41. Ladaoui W, Vidal T, Sellier A, Bourbon X (2013) Analysis of interactions between damage and basic creep of HPC and HPFRC heated between 20 and 80°C. *Mater Struct* 46:13–23
42. Vidal T, Sellier A, Ladaoui W, Bourbon X (2014) Effect of temperature on the basic creep of high-performance concretes heated between 20 and 80°C. *J Mater Civ Eng* B4014002
43. Aili A, Vandamme M, Torrenti JM, Masson B (2020) A viscoelastic poromechanical model for shrinkage and creep of concrete. *Cem Concr Res* 129:105970
44. Bazant ZP, Hauggaard AB, Baweja S, Ulm J (1997) Microprestressing-solidification theory for concrete creep. I: aging and drying effects. *J Eng Mech* 123:1188–1194
45. Lassabatère T, Torrenti JM, Granger L (1997) Sur le couplage entre séchage du béton et contrainte appliquée. *Actes du Colloque Saint-Venant, Paris, France*, 331–338
46. Neville AM (2000) *Propriétés des bétons*. Eyrolles, Paris
47. Rossi P, Tailhan JL, Maou FL, Gaillet L, Martin E (2012) Basic creep behavior of concretes investigation of the physical mechanisms by using acoustic emission. *Cem Concr Res* 42:61–73
48. Bazant ZP, Sener S, Kim JK (1986) Effect of cracking on drying permeability and diffusivity of concrete. *ACI Mater J* 84:351–357
49. Acker FJ (2001) Ulm, creep and shrinkage of concrete: physical origins and practical measurements. *Nucl Eng Des* 203:143–158
50. Sicard V, François R, Ringot E, Pons G (1992) Influence of creep and shrinkage on cracking in high strength concrete. *Cem Concr Res* 22:159–168
51. Bisschop J, Van Mier JGM (2002) Effect of aggregates on drying shrinkage microcracking in cement-based composites. *Mater Struct* 35:453–461
52. Ladaoui W (2010) *Étude expérimentale du comportement Thermo-Hydro-Mécanique à long terme des BHP destinées aux ouvrages de stockage des déchets radioactifs*, Doctoral thesis, University of Toulouse

**Publisher's Note** Springer Nature remains neutral with regard to jurisdictional claims in published maps and institutional affiliations.

